

# Inference of COVID-19 epidemiological distributions from Brazilian hospital data

Iwona Hawryluk,<sup>1</sup> Thomas A. Mellan,<sup>1,\*</sup> Henrique H Hoeltgebaum,<sup>2</sup> Swapnil Mishra,<sup>1</sup> Ricardo P Schnekenberg,<sup>3</sup> Charles Whittaker,<sup>1</sup> Harrison Zhu,<sup>2</sup> Axel Gandy,<sup>2</sup> Christl A. Donnelly,<sup>1,4</sup> Seth Flaxman,<sup>2,†</sup> and Samir Bhatt<sup>1</sup>

<sup>1</sup>*MRC Centre for Global Infectious Disease Analysis,  
Department of Infectious Disease Epidemiology, Imperial College London, UK*

<sup>2</sup>*Department of Mathematics, Imperial College London, UK*

<sup>3</sup>*Nuffield Department of Clinical Neurosciences, University of Oxford, UK*

<sup>4</sup>*Department of Statistics, University of Oxford, UK*

(Dated: August 25, 2020)

Knowing COVID-19 epidemiological distributions, such as the time from patient admission to death, is directly relevant to effective primary and secondary care planning, and moreover, the mathematical modelling of the pandemic generally. We determine epidemiological distributions for patients hospitalised with COVID-19 using a large dataset ( $N = 21,000 - 157,000$ ) from the Brazilian Sistema de Informao de Vigilncia Epidemiolgica da Gripe database. A joint Bayesian subnational model with partial pooling is used to simultaneously describe the 26 states and one federal district of Brazil, and shows significant variation in the mean of the symptom-onset-to-death time, with ranges between 11.2-17.8 days across the different states, and a mean of 15.2 days for Brazil. We find strong evidence in favour of specific probability density function choices: for example, the gamma distribution gives the best fit for onset-to-death and the generalised log-normal for onset-to-hospital-admission. Our results show that epidemiological distributions have considerable geographical variation, and provide the first estimates of these distributions in a low and middle-income setting. At the subnational level, variation in COVID-19 outcome timings are found to be correlated with poverty, deprivation and segregation levels, and weaker correlation is observed for mean age, wealth and urbanicity.

Keywords: COVID-19, Brazil, symptom-onset-to-death, admission-to-death, model selection

## 1. INTRODUCTION

Surveillance of COVID-19 has progressed from initial reports on 31st-Dec-2019 of pneumonia with unknown etiology in Wuhan, China,<sup>1</sup> to the confirmation of 9,826 cases of SARS-CoV-2 across 20 countries one month later,<sup>2</sup> to the current pandemic of greater than 12 million confirmed cases and 500,000 deaths globally to date.<sup>3</sup> Early estimates of epidemiological distributions provided critical input that enabled modelling to identify the severity and infectiousness of the disease. The onset-to-death distribution,<sup>4,5</sup> characterising the range of times observed between the onset of first symptoms in a patient and their death, has for example proved crucial in early estimates of the Infection Fatality Ratio (IFR),<sup>6</sup> and was similarly integral to recent approaches to modelling the transmission dynamics of SARS-CoV-2.<sup>7-12</sup>

Initial estimates of COVID-19 epidemiological distributions necessarily relied on relatively few data points, with the events comprising these distributions occurring a period of time that was short compared to the temporal pathologies of the disease progression, resulting in wide confidence or credible intervals and a sensitivity to time-series censoring effects.<sup>6</sup> Global surveillance of the disease over the past 197 days has provided more data to re-evaluate the time-delay distributions of

the disease. In particular, public availability of a large number of patient-level hospital records – currently over 390,000 in total – from the SIVEP-Gripe (*Sistema de Informao de Vigilncia Epidemiolgica da Gripe*) database published by Brazil’s Ministry of Health (MoH),<sup>13</sup> provides an opportunity to make robust statistical estimates of the onset-to-death and other time-delay distributions such as onset-to-diagnosis, length of ICU stay, onset-to-hospital-admission, onset-to-hospital-discharge, onset-to-ICU-admission, and hospital-admission-to-death. In this work we fit and present an analysis of these epidemiological distributions, with the paper set out as follows. Section 2 describes the data used from the SIVEP-Gripe database,<sup>13</sup> and the methodological approach applied to fit distributions using a hierarchical Bayesian model with partial pooling. Section 3 provides a description of the results from this study from fitting epidemiological distributions at national and subnational level to a range of probability density functions (PDFs). The results are discussed in Section 4, including associations with socioeconomic factors, such as education, segregation, and poverty, and conclusions are given in Section 5.

## 2. METHODS

### 2.1. Data

The SIVEP-Gripe database provides detailed patient-level records for all individuals hospitalised with severe acute respiratory syndrome, including all suspected or

\* t.mellan@imperial.ac.uk

† s.flaxman@imperial.ac.uk

confirmed cases of severe COVID-19.<sup>13</sup> The records include the date of admission, date of onset of symptoms, state where the patient lives, state where they are being treated, and date of outcome (death or discharge), among other diagnosis related variables. We extracted the data for confirmed COVID-19 records starting on 25th February and considered records in our analysis ending on 7th July. The dataset was filtered to obtain rows for onset-to-death, hospital-admission-to-death, length of ICU stay, onset-to-hospital-admission, onset-to-hospital-discharge, onset-to-ICU-admission and onset-to-diagnosis. Onset-to-diagnosis data were split into the diagnosis confirmed by PCR and those confirmed by other methods, such as rapid antibody and antigen tests, called non-PCR throughout this manuscript. Entries resulting in distribution times greater than 133 days were considered a typing error and removed, as the first recorded COVID-19 case in Brazil was on 25th February.<sup>14</sup>

Additional filtering of the data was applied for onset-to-ICU-admission, onset-to-hospital-admission and onset-to-death in order to eliminate bias introduced by potentially erroneous entries identified in the data for these distributions. We removed the rows where admission to the hospital or ICU or death happened on the same day as onset of symptoms, assuming that these were actually incorrectly inputted entries. The decision to test removing the first day is motivated firstly by the observation of a number of conspicuous data entry errors in the database, and secondly by anomalous spikes corresponding to same-day events observed in these distributions. An example of the anomalous spikes in the onset-to-death distribution is shown in Appendix Figure 4 for selected states.

Sensitivity analyses on data inclusion, regarding the removal of anomalous spikes in first-day data indicative of reporting errors (e.g. in onset to hospital admission), and regarding the sensitivity of the dataset to time-series censoring effects, are set out in the Results Section 3.3.

A summary of the data, including number and a range of samples per variable from the SIVEP-Gripe dataset is given in Table I. A breakdown of the number of data samples per state is provided in Appendix Table IX.

Basic exploratory analysis to explain geographic variation observed in time-delay distributions adopts *GeoSES* (*ndice Socioeconmico do Contexto Geogrfico para Estudos em Sade*),<sup>15</sup> which measures Brazilian socioeconomic characteristics through an index composed of education, mobility, poverty, wealth, deprivation, and segregation. We investigate correlations between the *GeoSES* indicators and the time-delay means that we estimate at the state level. Additionally, we consider correlations with the mean age of the population of the state and the percentage of people living in urban areas, data we obtained from *Instituto Brasileiro de Geografia e Estatstica* (*IBGE*).<sup>16</sup>

Table I. Summary of the distribution data extracted from SIVEP-Gripe database.<sup>13</sup> Number of samples ( $N_{\text{samples}}$ ) is given for the whole country.

Distribution	$N_{\text{samples}}$	Range (days)
Onset-to-death	59,271	1-114
Hospital-admission-to-death	52,821	0-99
ICU-stay	21,709	0-89
Onset-to-hospital-admission	141,618	1-129
Onset-to-hospital-discharge	69,478	0-120
Onset-to-ICU-admission	46,617	0-101
Onset-to-diagnosis (PCR)	156,558	0-129
Onset-to-diagnosis (non-PCR)	19,438	0-102

## 2.2. Model fitting

Gamma, Weibull, log-normal, generalised log-normal,<sup>17</sup> and generalised gamma<sup>18</sup> PDFs are fitted to several epidemiological distributions, with the specific parameterisations provided in Appendix Section 10.1. The parameters of each distribution are fitted in a joint Bayesian hierarchical model with partial pooling, using data from the 26 states and one federal district of Brazil, extracted and filtered to identify specific epidemiological distributions such as onset-to-death, ICU-stay, and so on.

As an example consider fitting a gamma PDF for the onset-to-death distribution. The gamma distribution for the  $i^{\text{th}}$  state is given by

$$\text{Gamma}(\alpha_i, \beta_i), \quad (1)$$

where shape and scale parameters are assumed to be positively constrained, normally distributed random variables

$$\alpha_i \sim N(\alpha_{\text{Brazil}}, \sigma_1) \quad (2)$$

and

$$\beta_i \sim N(\beta_{\text{Brazil}}, \sigma_2). \quad (3)$$

The parameters  $\alpha_{\text{Brazil}}$  and  $\beta_{\text{Brazil}}$  denote the national level estimates, and

$$\sigma_1 \sim N^+(0, 1), \sigma_2 \sim N^+(0, 1), \quad (4)$$

where  $N^+(\cdot)$  is a truncated normal distribution. In this case, parameters  $\alpha_{\text{Brazil}}$  and  $\beta_{\text{Brazil}}$  are estimated by fitting a gamma PDF to the fully pooled data, that is including the observations for all states. Prior probabilities for the national level parameters for each of the considered PDFs are chosen to be  $N^+(0, 1)$ , except for the generalised gamma distribution where we used:  $\mu_{\text{Brazil}} \sim N^+(2, 0.5)$ ,  $\sigma_{\text{Brazil}} \sim N^+(0.5, 0.5)$  and  $s_{\text{Brazil}} \sim N^+(1.5, 0.5)$ .

Posterior samples of the parameters in the model are generated using Hamiltonian Monte Carlo (HMC) with Stan.<sup>19,20</sup> For each fit we use 4 chains and 2,000 iterations, with half of the iterations dedicated to warm-up.

The preference for one fitted model over another is characterised in terms of the Bayesian support, with the model evidence calculated to see how well a given model fits the data, and comparison between two models using Bayes Factors. The details of how to estimate the model evidence and calculate the Bayes Factors for each pair of models are given in Appendix Section 10.1.

### 3. RESULTS

#### 3.1. Brazil epidemiological distributions

Five trial PDFs – gamma, Weibull, log-normal, generalised log-normal and generalised gamma – were fitted to the epidemiological data shown in Figure 1.

All of the models’ fits were tested by using the Bayes Factors based on the Laplace approximation and corrected using thermodynamic integration,<sup>21–23</sup> as described in Appendix Section 10.1. The thermodynamic integration contribution was negligible suggesting the posterior distributions are satisfactorily approximated as multivariate normal. The conclusions on the preferred PDF were not sensitive to the choice of prior distributions, that is the preferred model was still the favoured one even when more informative prior distributions were applied for all PDFs. The Bayes Factors used for model selection are shown in Appendix Table V.

The gamma PDF provided the best fit to the onset-to-death, hospital-admission-to-death and ICU-stay data. For the remaining distributions – onset-to-diagnosis (non-PCR), onset-to-diagnosis (PCR), onset-to-hospital-discharge, onset-to-hospital-admission and onset-to-ICU-admission – the generalised log-normal distribution was the preferred model. The list of preferred PDFs for each distribution, together with the estimated mean, variance and PDFs’ parameter values for the national fits are given in Table II. The 95% credible intervals (CrI) for parameters of each of the preferred PDFs was less than 0.1 wide, therefore in Table II we show only point estimates.

Additionally, in Figure 1, in each instance the cumulative probability distribution is given for the best model fit, revealing that out of patients for whom COVID-19 is terminal, almost 70% die within 20 days of symptom onset. Out of patients who die in the hospital, almost 60% die within the first 10 days since admission.

The estimated mean number of days for each distribution for Brazil is compared in Table III with values found in the literature for China, US and France. The majority of the data obtained through searching the literature pertained to the early stages of the epidemic in China, and no data was found for low- and middle-income countries. The mean onset-to-death time of 15.2 (95% CrI 15.1 – 15.3) days, from a best-fitting gamma PDF, is shorter than the 17.8 (95% CrI 16.9–19.2) days estimate from Verity et al.,<sup>6</sup> and 20.2 (95% CrI 15.1 – 29.5) days estimate (14.5 days without truncation) from Linton et al.<sup>12</sup> In both cases, estimates were based on a small sam-

ple size from the beginning of the epidemic in China. The mean number of days for hospital-admission-to-death of 10.8 (95% CrI 10.7 – 10.9) for Brazil matches closely the 10 days estimated by Salje et al.<sup>24</sup>

#### 3.2. Subnational Brazilian epidemiological distributions

The onset-to-death distribution, and other time-delay distributions such as onset-to-diagnosis, length of ICU stay, onset-to-hospital-admission, onset-to-hospital-discharge, onset-to-ICU-admission, and hospital-admission-to-death, have been fitted in a joint model across the 26 states and one federal district of Brazil using partial pooling. The mean number of days, plotted in Figure 2, shows substantial subnational variability – e.g. the mean onset-to-hospital-admission for Amazonas state was estimated to be 9.9 days (95% CrI 9.7–10.1), whereas for Mato Grosso do Sul the estimate was 6.7 (95% CrI 6.4–7.1) days and Rio de Janeiro - 7.2 days (95% CrI 7.1–7.3). Amazonas state had the longest average time from onset-to-hospital-and ICU-admission. The state with the shortest average onset-to-death time was Acre. Santa Catarina state on the other hand had a longest average onset-to-death and hospital-admission-to-death time, as well as longest average ICU-stay. For a visualisation of the uncertainty in our mean estimates for each state, see the posterior density plots in Appendix Figures 5 and 6. Additional national and state-level results for the onset-to-death gamma PDF, including the posterior plots for mean and variance, are shown in Figure 7 in the Appendix.

We also observe discrepancies between the five geographical regions of Brazil, for example states belonging to the southern part of the country (Paraná, Rio Grande do Sul and Santa Catarina) had a longer average ICU-stay and hospital-admission-to-death time as compared to the states in the North region. Full results, including detailed estimates of mean, variance, and estimates for each of the distributions’ parameters for Brazil and Brazilian states can be accessed at [https://github.com/mrc-ide/Brazil\\_COVID19\\_distributions/blob/master/results/results\\_full\\_table.csv](https://github.com/mrc-ide/Brazil_COVID19_distributions/blob/master/results/results_full_table.csv).

#### 3.3. Sensitivity analyses

In order to remove the potential bias towards shorter outcomes from left- and right-censoring, we tested the scenario in which the data to fit the models was truncated. For example, based on a 95% quartile of 35 days for the hospital-admission-to-death distribution, entries with the starting date (hospital admission) after 2nd June 2020 and those with an end-date (death) before 1st April were truncated, and the models were refitted. With censored parts of the data removed, the mean time from start to outcome increased for every distribution, e.g. for

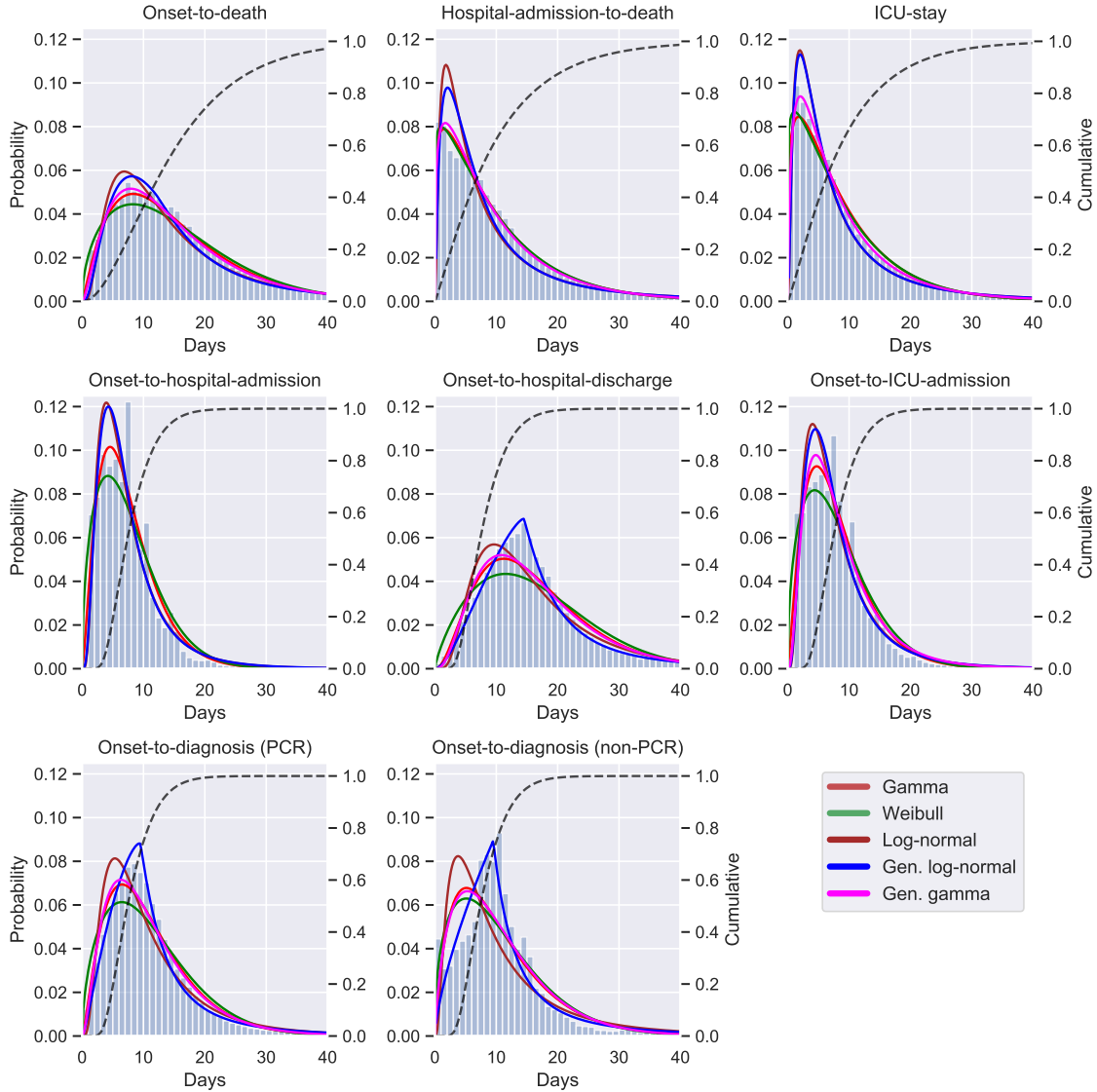


Figure 1. Histograms for onset-to-death, hospital-admission-to-death, ICU-stay, onset-to-hospital-admission, onset-to-hospital-discharge, onset-to-ICU-admission, onset-to-diagnosis (PCR) and onset-to-diagnosis (non-PCR) distributions show data for Brazil extracted from the SIVEP-Gripe database.<sup>13</sup> For each distribution, solid lines are for fitted PDFs and the dashed line shows the cumulative distribution function of the best-fitting PDF. The left hand side y-axis gives the probability value for the PDFs and the right hand side y-axis shows the value for the cumulative distribution function. All values on the x-axes are given in days. State-level fits are shown in Figure 2 and Appendix Figures 5 and 6.

hospital-admission-to-death it increased from 10.0 (95% CrI 9.9-10.0) to 10.8 (95 % CrI 10.7-10.9), and for onset-to-death it changed from 15.2 days (95% CrI 15.1-15.3) to 16.0 days (95% CrI 15.9-16.1). The effect truncation on censored data is given in Appendix Figure 8.

To test the impact of keeping or removing entries identified as potentially resulting from erroneous data transcription (see the Methods Section 2), we fitted the PDFs to some of the distributions on a national level with and without those entries. For onset-to-hospital-admission, onset-to-ICU and onset-to-death we find that generalised gamma PDF was preferred when the first day

of the distribution was included, and gamma (for onset-to-death) and generalised log-normal PDFs if the first day was removed. For hospital-admission-to-death, a gamma distribution fitted most accurately when the first day was included, and Weibull when it was excluded. The effect of removing the first day results in means shifting to the right by approximately 1 day for both onset-to-hospital- and ICU-admission, and by 0.5 days for hospital-admission-to-death (see Appendix Figure 8).

Sensitivity analysis regarding the model selection approach is detailed in Appendix Section 10.1.

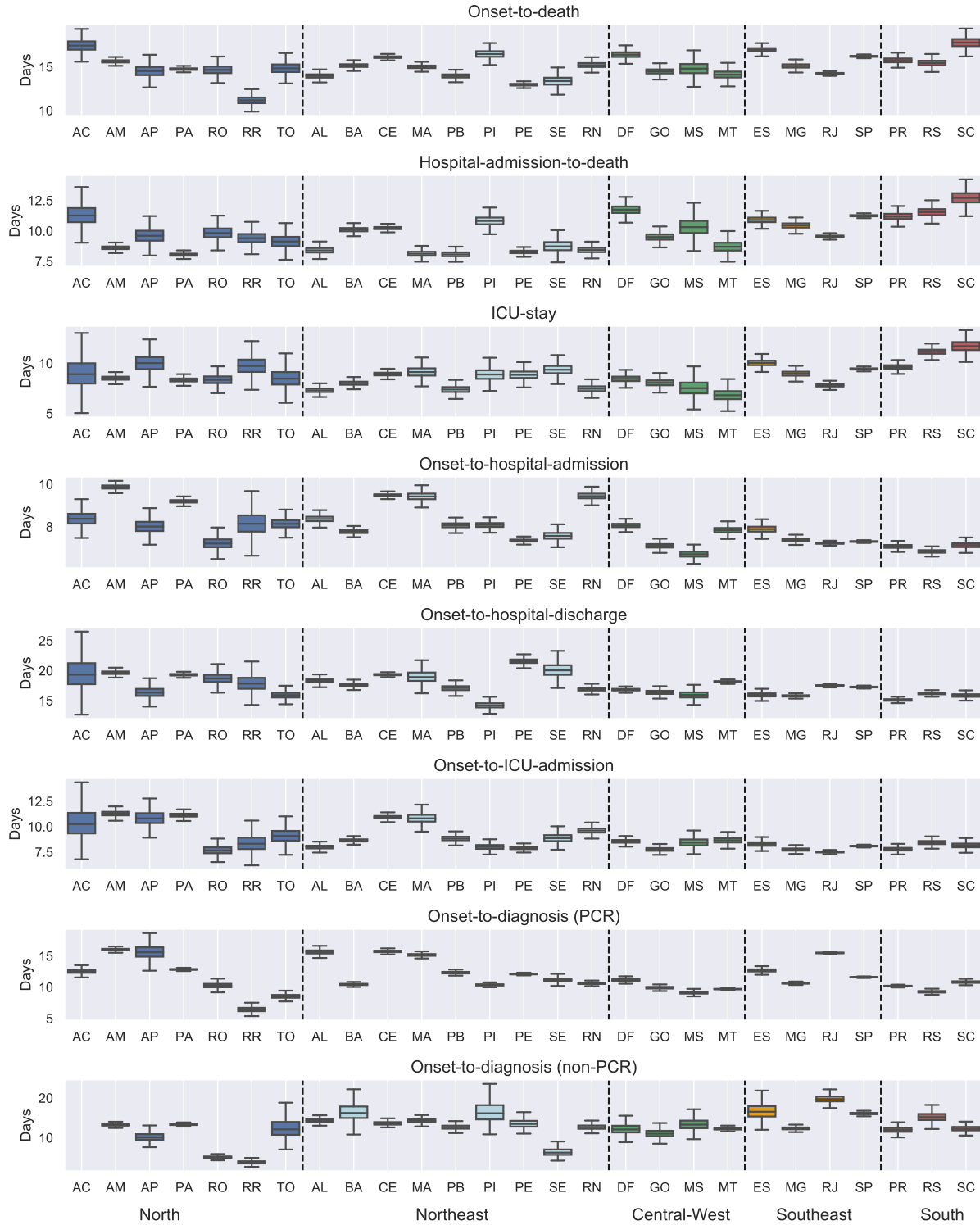


Figure 2. Estimates of the mean time in days for onset-to-death, hospital-admission-to-death and each of the other distributions fitted in the joint model of Brazil. Estimates are grouped by the five regions of Brazil, North (blue), Northeast (light-blue), Central-West (green), Southeast (orange), South (red), and are shown for Acre (AC), Amazonas (AM), Amap (AP), Par (PA), Rondnia (RO), Roraima (RR), Tocantins (TO), Alagoas (AL), Bahia (BA), Cear (CE), Maranh (MA), Paraba (PB), Piau (PI), Pernambuco (PE), Sergipe (SE), Rio Grande do Norte (RN), Distrito Federal (DF), Gois (GO), Mato Grosso do Sul (MS), Mato Grosso (MT), Espirito Santo (ES), Minas Gerais (MG), Rio de Janeiro (RJ), So Paulo (SP), Paran (PR), Rio Grande do Sul (RS), Santa Catarina (SC). For state Acre, the onset-to-diagnosis (non-PCR) mean diverged due to the small number of samples ( $n=1$ ). The full posterior distribution for each mean estimate is given in Appendix Figures 5 and 6.

Table II. For each COVID-19 distribution the preferred PDF with the largest Bayesian support is listed, along with the estimated mean, variance and other parameter of the PDF. 95% credible intervals are given in brackets for mean and variance. The parameters  $p_1$ ,  $p_2$  and  $p_3$  for the preferred PDFs gamma and generalised log-normal (GLN) are given in the form  $\text{Gamma}(x|p_1, p_2) = \text{Gamma}(\alpha, \beta)$  and  $\text{GLN}(x|p_1, p_2, p_3) = \text{GLN}(\mu, \sigma, s)$ , with the formulae of the PDFs given in Appendix Section 10. The credible intervals for parameters  $p_1$ ,  $p_2$  and  $p_3$  are less than 0.1 wide, so only the point estimates are shown. † The variance diverges for the onset-to-diagnosis (non-PCR) PDF.

Distribution	Preferred PDF	Mean (days)	Variance (days <sup>2</sup> )	$p_1$	$p_2$	$p_3$
Onset-to-death	Gamma	15.2 (15.1, 15.3)	105.3 (103.7, 106.9)	2.2	0.1	-
Hospital-admission-to-death	Gamma	10.0 (9.9, 10.0)	84.8 (83.2, 86.4)	1.2	0.1	-
ICU-stay	Gamma	9.0 (8.9, 9.1)	64.9 (63.1, 66.8)	1.2	0.1	-
Onset-to-hospital-admission	Gen. log-normal	7.8 (7.7, 7.8)	35.7 (35.0, 36.5)	1.8	0.6	1.8
Onset-to-hospital-discharge	Gen. log-normal	17.6 (17.6, 17.7)	248.7 (233.7, 265.6)	2.7	0.3	1.2
Onset-to-ICU-admission	Gen. log-normal	8.5 (8.4, 8.5)	48.0 (46.1, 50.0)	1.9	0.6	1.8
Onset-to-diagnosis (PCR)	Gen. log-normal	12.5 (12.5, 12.6)	252.3 (236.4, 269.6)	2.3	0.3	1.2
Onset-to-diagnosis (non-PCR)	Gen. log-normal	14.5 (14.3, 14.7)	†	2.3	0.3	1.0

Table III. Epidemiological distributions for COVID-19 have been fitted for Brazil, and sources worldwide have been obtained from the literature. PDF means for Brazil have been obtained using Markov Chain Monte Carlo (MCMC) sampling, using the PDF with the maximum Bayesian support for each data distribution (see Appendix Table V). All values are given in days, and 95% CrI are given in brackets unless stated otherwise. \* adjusted for censoring, † PCR confirmed, ‡ non-PCR confirmed, <sup>a</sup> median (interquartile range), <sup>b</sup> mean (standard deviation).

Distribution	Brazil	China	France	US
Onset-to-death	15.2 (15.1, 15.3) 16.0* (15.9, 16.1)	17.8 (16.9, 19.2) <sup>6</sup>	10.0 <sup>27</sup>	13.59 <sup>b</sup> (7.85) <sup>25</sup>
		18.8* (15.7, 49.7) <sup>6</sup>		
		14.5 (12.5, 17.0) <sup>12</sup>		
		20.2* (15.1, 29.5) <sup>12</sup>		
Hospital-admission-to-death	10.0 (9.9, 10.0) 10.8* (10.7, 10.9)	5.0 <sup>a</sup> (3.0, 9.3) <sup>26</sup>	10.0 <sup>27</sup>	
		8.9 (7.3-10.4) <sup>12</sup>		
		13.0* (8.7-20.9) <sup>12</sup>		
ICU-stay	9.0 (8.9, 9.1) 10.1* (9.9, 10.2)	8.0 <sup>a</sup> (4.0, 12.0) <sup>28</sup>	17.6 (17.0, 18.2) <sup>27</sup>	
Onset-to-hospital-admission	7.8 (7.7, 7.8)	10.0 <sup>a</sup> (7.0-12.0) <sup>26</sup>		
Onset-to-hospital-discharge	17.6 (17.6, 17.7)	22.0 <sup>a</sup> (18.0, 25.0) <sup>28</sup>		
Onset-to-ICU-admission	8.5 (8.4, 8.5)	9.5 <sup>a</sup> (7.0, 12.5) <sup>29</sup>		
Onset-to-diagnosis	12.5†(12.5, 12.6)	5.5 (5.4, 5.7) <sup>24</sup>		
	14.5‡(14.3, 14.7)			

#### 4. DISCUSSION

We fitted multiple probability density functions to a number of epidemiological datasets, such as onset-to-death or onset-to-diagnosis, from the Brazilian SIVEP Gripe database,<sup>13</sup> using Bayesian hierarchical models. Our findings provide the first reliable estimates of the various epidemiological distributions for the COVID-19 epidemic in Brazil and highlight a need to consider a wider set of specific parametric distributions. Instead of relying on the ubiquitous gamma or log-normal distributions, we show that often these PDFs do not best capture the behaviour of the data. For instance, the generalised log-normal is preferable for several of the epidemiological distributions in Table II. These results can inform modelling of the epidemic in Brazil,<sup>30</sup> and other low- and middle-income countries,<sup>31</sup> but we expect they also have some relevance more generally.

In terms of modelling the epidemic in Brazil, the variation observed at subnational level – see Figure 2 – can be

shown to be important to accurately estimating disease progression. Making use of the state-level custom-fitted onset-to-death distributions reported here, we have estimated the number of active infections on 23rd June 2020 across ten states spanning the five regions of Brazil, using a Bayesian hierarchical renewal-type model.<sup>7,30,32</sup> The relative change in the number of active infections from modelling the cases using heterogeneous state-specific onset-to-death distributions, compared to using a single common Brazil one is shown in Figure 3 to be quite substantial. The relative changes observed, up to 18% more active infections, suggest assumptions of onset-to-death homogeneity are unreliable and closer attention needs to be paid when fitting models of SARS-CoV-2 transmission dynamics in large countries.

On the origin of the geographic variation displayed in Figure 2 for the average distribution times across states, there are multiple potential factors that could generate the observed variability and in this work we present an elementary exploratory analysis. We exam-

ine the correlation between socioeconomic factors, such as education, poverty, income, etc., using a number of socioeconomic state-level indicators obtained from Barrozo et al.(2020)<sup>15</sup> and additional datasets containing the mean age per state and percentage of people living in the urban areas (urbanicity).<sup>16</sup> The Pearson correlation coefficients, shown in the Appendix Table VII, suggest that segregation, poverty and deprivation elements were most strongly correlated with the analysed onset-time datasets. E.g. poverty was strongly negatively correlated with hospital-admission-to-death (-0.68), whereas income and segregation had a high positive correlation coefficient for the same distribution (+0.60, +0.62 respectively). The strongest correlation was observed for hospital-admission-to-death and deprivation indicator, which measures the access to sanitation, electricity and other material and non-material goods.<sup>15</sup> Interestingly, the indicators measuring economical situation were more correlated with average hospitalisation times than mean age per state, which suggests that although the low- and middle-income countries typically have younger populations, their healthcare systems are more likely to struggle in response to the COVID-19 epidemic. More detailed analysis is necessary to fully appreciate the impact of the economic components on the COVID-19 epidemic response.

In the work presented we acknowledge numerous limitations. The database from which distributions have been extracted, though extensive, contains transcription errors, and the degree to which these bias our estimates is largely unknown. Secondly, the PDFs fitted are based on observational hospital data, and therefore should be cautiously interpreted for other settings. Thirdly, though we have fitted PDFs at subnational as well as national level, this partition is largely arbitrary and further work is re-

quired to understand the likely substantial effect of age, sex, ethnic variation,<sup>33</sup> co-morbidities, and other factors.

## 5. CONCLUSIONS

We provide the first estimates of common epidemiological distributions for the COVID-19 epidemic in Brazil, based on the SIVEP-Gripe hospitalisation data.<sup>13</sup> Extensive heterogeneity in the distributions between different states is reported. Quantifying the time-delay for COVID-19 onset and hospitalisation data provides useful input parameters for many COVID-19 epidemiological models, especially those modelling the healthcare response in low- and middle-income countries.

## 6. ACKNOWLEDGEMENTS

We thank Microsoft for providing Azure credits which were used to run the analysis.

## 7. FUNDING

This work was supported by Centre funding from the UK Medical Research Council under a concordat with the UK Department for International Development, the NIHR Health Protection Research Unit in Modelling Methodology and Community Jameel. This research was also partly funded by the Imperial College COVID-19 Research Fund. IH was supported by Imperial College London MRC Centre.

## 8. CODE AND DATA AVAILABILITY

Python, R and Stan code used to analyse the data and fit the distribution is available at [https://github.com/mrc-ide/Brazil\\_COVID19\\_distributions](https://github.com/mrc-ide/Brazil_COVID19_distributions), along with estimated parameters for each state and PDFs considered at [https://github.com/mrc-ide/Brazil\\_COVID19\\_distributions/blob/master/results/results\\_full\\_table.csv](https://github.com/mrc-ide/Brazil_COVID19_distributions/blob/master/results/results_full_table.csv). The SIVEP-Gripe database,<sup>13</sup> is available to download from Brazil Ministry of Health website <https://opendatasus.saude.gov.br/dataset/bd-srag-2020>.

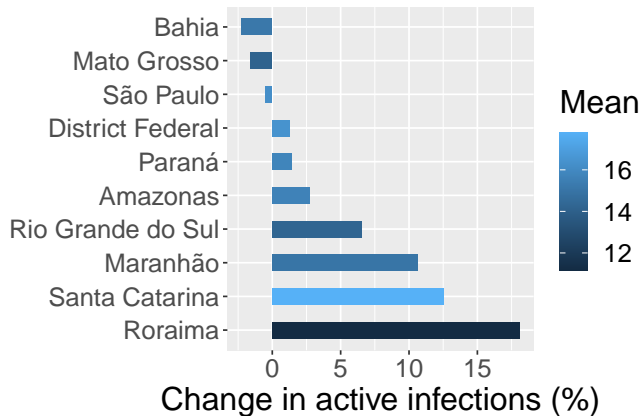


Figure 3. This figure shows the percentage change in active infections, estimated on the 23rd-Jun-2020, that results from using state-specific onset-to-death distributions (see Appendix Table VI) compared to a single national-level one. The effect for each state is coloured according to the mean of the state’s onset-to-death gamma distribution, given in days. The mean onset-to-death for Brazil is 15.2 days.

## 9. REFERENCES

- <sup>1</sup> World Health Organisation, WHO, Coronavirus disease 2019 (COVID-19) Situation Report 1, (2020).
- <sup>2</sup> World Health Organisation, WHO, Coronavirus disease 2019 (COVID-19) Situation Report 11, (2020).
- <sup>3</sup> World Health Organisation, WHO, Coronavirus disease 2019 (COVID-19) Situation Report 175, (2020).
- <sup>4</sup> C. A. Donnelly, A. C. Ghani, G. M. Leung, A. J. Hedley, C. Fraser, S. Riley, L. J. Abu-Raddad, L.-M. Ho, T.-Q. Thach, P. Chau, K.-P. Chan, L.-Y. T. Tai-Hing Lam, S.-H. L. Thomas Tsang, E. M. C. L. James H B Kong, N. M. Ferguson, and R. M. Anderson, Epidemiological determinants of spread of causal agent of severe acute respiratory syndrome in Hong Kong, *The Lancet* **361**, 1761 (2003).
- <sup>5</sup> T. Garske, J. Legrand, C. A. Donnelly, H. Ward, S. Cauchemez, C. Fraser, N. M. Ferguson, and A. C. Ghani, Assessing the severity of the novel influenza A/H1N1 pandemic, *BMJ* **339**, 10.1136/bmj.b2840 (2009), <https://www.bmj.com/content>.
- <sup>6</sup> R. Verity, L. C. Okell, I. Dorigatti, P. Winskill, C. Whitaker, N. Imai, G. Cuomo-dannenburg, H. Thompson, P. G. T. Walker, H. Fu, A. Dighe, T. Jamie, K. Gaythorpe, W. Green, A. Hamlet, W. Hinsley, D. Laydon, and G. Nedjati, Estimates of the severity of COVID-19 disease, *Lancet Infect Dis* **20**, [https://doi.org/10.1016/S1473-3099\(20\)30243-7](https://doi.org/10.1016/S1473-3099(20)30243-7) (2020).
- <sup>7</sup> S. Flaxman, S. Mishra, A. Gandy, H. J. T. Unwin, H. Coupland, T. A. Mellan, H. Zhu, T. Berah, J. W. Eaton, I. C. R. Team, A. Ghani, C. A. Donnelly, S. Riley, L. C. Okell, M. A. C. Vollmer, N. M. Ferguson, and S. Bhatt, Estimating the effects of non-pharmaceutical interventions on COVID-19 in Europe, *Nature*, 1 (2020).
- <sup>8</sup> J. T. Wu, K. Leung, N. K. Mary Bushman, R. Niehus, P. M. de Salazar, B. J. Cowling, M. Lipsitch, and G. M. Leung, First-wave COVID-19 transmissibility and severity in China outside Hubei after control measures, and second-wave scenario planning: a modelling impact assessment, *The Lancet* **395**, 1382 (2020).
- <sup>9</sup> S. Dana, A. B. Simas, B. A. Filardi, R. N. Rodriguez, L. L. da Costa Valiengo, and J. Gallucci-Neto, Brazilian Modeling of COVID-19 (bram-cod): a Bayesian Monte Carlo approach for COVID-19 spread in a limited data set context, *medRxiv* (2020).
- <sup>10</sup> J. T. Wu, K. Leung, N. K. Mary Bushman, R. Niehus, B. J. C. Pablo M. de Salazar, M. Lipsitch, and G. M. Leung, Estimating clinical severity of COVID-19 from the transmission dynamics in Wuhan, China, *Nature Medicine* **26**, 506510 (2020).
- <sup>11</sup> T. Jombart, K. Van Zandvoort, T. W. Russell, C. I. Jarvis, A. Gimma, S. Abbott, S. Clifford, S. Funk, H. Gibbs, Y. Liu, *et al.*, Inferring the number of COVID-19 cases from recently reported deaths, *Wellcome Open Research* **5** (2020).
- <sup>12</sup> N. M. Linton, T. Kobayashi, Y. Yang, K. Hayashi, A. R. Akhmetzhanov, S.-m. Jung, B. Yuan, R. Kinoshita, and H. Nishiura, Incubation period and other epidemiological characteristics of 2019 novel coronavirus infections with right truncation: a statistical analysis of publicly available case data, *Journal of clinical medicine* **9**, 538 (2020).
- <sup>13</sup> SRAG 2020 - Banco de Dados de Sndrome Respiratria Aguda Grave, (2020).
- <sup>14</sup> Editorial, COVID-19 in Brazil: "so what?", *The Lancet* **10.1016/S0140-6736(20)31095-3** (2020).
- <sup>15</sup> L. V. Barrozo, M. Fornaciali, C. D. S. de Andr, G. A. Z. Morais, G. Mansur, W. Cabral-Miranda, M. J. de Miranda, J. R. Sato, and E. A. Jnior, GeoSES: A socioeconomic index for health and social research in Brazil, *PLoS ONE* **15**, <https://doi.org/10.1371/journal.pone.0232074> (2020).
- <sup>16</sup> Brazilian Institute of Geography and Statistics, Ibge Projees da Populao, .
- <sup>17</sup> B. Singh, K. K. Sharma, S. Rathi, and G. Singh, A generalized log-normal distribution and its goodness of fit to censored data, *Computational Statistics* **27**, 5167 (2012).
- <sup>18</sup> E. W. Stacy *et al.*, A generalization of the gamma distribution, *The Annals of mathematical statistics* **33**, 1187 (1962).
- <sup>19</sup> B. Carpenter, A. Gelman, M. D. Hoffman, D. Lee, B. Goodrich, M. Betancourt, M. Brubaker, J. Guo, P. Li, and A. Riddell, Stan: A probabilistic programming language, *Journal of statistical software* **76** (2017).
- <sup>20</sup> M. D. Hoffman and A. Gelman, The No-U-Turn sampler: adaptively setting path lengths in Hamiltonian Monte Carlo, *J. Mach. Learn. Res.* **15**, 1593 (2014).
- <sup>21</sup> T. A. Mellan, I. Hawryluk, S. Mishra, and S. Bhatt, Simulating normalising constants using referenced thermodynamic integration, In preparation (2020).
- <sup>22</sup> X.-L. Meng and W. H. Wong, Simulating ratios of normalizing constants via a simple identity: a theoretical exploration, *Statistica Sinica*, 831 (1996).
- <sup>23</sup> A. Gelman and X.-L. Meng, Simulating normalizing constants: From importance sampling to bridge sampling to path sampling, *Statistical science*, 163 (1998).
- <sup>24</sup> M. Li, P. Chen, Q. Yuan, B. Song, and J. Ma, Transmission characteristics of the COVID-19 outbreak in China: a study driven by data, preprint (2020).
- <sup>25</sup> E. Abdollahi, D. Champredon, J. M. Langley, A. P. Galvani, and S. M. Moghadas, Temporal estimates of case-fatality rate for COVID-19 outbreaks in Canada and the United States, *CMAJ* <https://doi.org/10.1503/cmaj.200711> (2020).
- <sup>26</sup> T. Chen, D. Wu, H. Chen, W. Yan, D. Yang, G. Chen, K. Ma, D. Xu, H. Yu, H. Wang, T. Wang, W. Guo, J. Chen, C. Ding, X. Zhang, J. Huang, M. Han, S. Li, X. Luo, J. Zhao, and Q. Ning, Clinical characteristics of 113 deceased patients with coronavirus disease 2019: retrospective study, *BMJ* **368**, 10.1136/bmj.m1091 (2020).
- <sup>27</sup> H. Salje, C. Tran Kiem, N. Lefrancq, N. Courtejoie, P. Bosetti, J. Paireau, A. Andronico, N. Hozé, J. Richet, C.-L. Dubost, Y. Le Strat, J. Lessler, D. Levy-Bruhl, A. Fontanet, L. Opatowski, P.-Y. Boelle, and S. Cauchemez, Estimating the burden of SARS-CoV-2 in France, *Science* **369**, 208 (2020).
- <sup>28</sup> F. Zhou, T. Yu, R. Du, G. Fan, Y. Liu, Z. Liu, J. Xiang, Y. Wang, B. Song, X. Gu, L. Guan, Y. Wei, H. Li, X. Wu, J. Xu, S. Tu, Y. Zhang, H. Chen, and B. Cao, Clinical



- course and risk factors for mortality of adult inpatients with COVID-19 in Wuhan, China: a retrospective cohort study, *The Lancet* 10.1016/S0140-6736(20)30566-3 (2020).
- <sup>29</sup> X. Yang, Y. Yu, J. Xu, H. Shu, J. Xia, H. Liu, Y. Wu, L. Zhang, Z. Yu, M. Fang, T. Yu, Y. Wang, S. Pan, X. Zou, S. Yuan, and Y. Shang, Clinical course and outcomes of critically ill patients with SARS-CoV-2 pneumonia in Wuhan, China: a single-centered, retrospective, observational study, *Lancet Respir Med* **8**, [https://doi.org/10.1016/S2213-2600\(20\)30079-5](https://doi.org/10.1016/S2213-2600(20)30079-5) (2020).
- <sup>30</sup> T. A. Mellan, H. H. Hoeltgebaum, S. Mishra, C. Whittaker, R. P. Schnekenberg, A. Gandy, H. J. T. Unwin, M. A. Vollmer, H. Coupland, I. Hawryluk, *et al.*, Report 21: Estimating COVID-19 cases and reproduction number in Brazil, *medRxiv* (2020).
- <sup>31</sup> P. G. T. Walker, C. Whittaker, O. J. Watson, M. Baguelin, P. Winskill, A. Hamlet, B. A. Djafaara, Z. Cucunubá, D. Olivera Mesa, W. Green, H. Thompson, S. Nayagam, K. E. C. Ainslie, S. Bhatia, S. Bhatt, A. Boonyasiri, O. Boyd, N. F. Brazeau, L. Cattarino, G. Cuomo-Dannenburg, A. Dighe, C. A. Donnelly, I. Dorigatti, S. L. van Elsland, R. FitzJohn, H. Fu, K. A. Gaythorpe, L. Geidelberg, N. Grassly, D. Haw, S. Hayes, W. Hinsley, N. Imai, D. Jorgensen, E. Knock, D. Laydon, S. Mishra, G. Nedjati-Gilani, L. C. Okell, H. J. Unwin, R. Verity, M. Vollmer, C. E. Walters, H. Wang, Y. Wang, X. Xi, D. G. Lalloo, N. M. Ferguson, and A. C. Ghani, The impact of COVID-19 and strategies for mitigation and suppression in low- and middle-income countries, *Science* 10.1126/science.abc0035 (2020).
- <sup>32</sup> S. Mishra, T. Berah, T. A. Mellan, H. J. T. Unwin, M. A. Vollmer, K. V. Parag, A. Gandy, S. Flaxman, and S. Bhatt, On the derivation of the renewal equation from an age-dependent branching process: an epidemic modelling perspective, *arXiv preprint arXiv:2006.16487* (2020).
- <sup>33</sup> P. Baqui, I. Bica, V. Marra, A. Ercole, and M. van der Schaar, Ethnic and regional variations in hospital mortality from COVID-19 in Brazil: a cross-sectional observational study, *The Lancet* [https://doi.org/10.1016/S2214-109X\(20\)30285-0](https://doi.org/10.1016/S2214-109X(20)30285-0) (2020).
- <sup>34</sup> L. Tierney and J. B. Kadane, Accurate approximations for posterior moments and marginal densities, *Journal of the American Statistical Association* **81**, 82 (1986).
- <sup>35</sup> R. E. Kass and R. Adrian E, Bayes Factors, *Journal of the American Statistical Association* **90**, 773 (1995), <https://www.stat.cmu.edu/kass/papers/bayesfactors.pdf>.

## 10. APPENDIX

### 10.1. Model selection

To characterise which model (gamma, log-normal, etc.) best fits the data, the Bayesian model evidence  $z = z(y|M_i)$  is evaluated. Here and throughout this section  $y$  denotes the data and  $M_i$  denotes the  $i^{\text{th}}$  model from the analysed model set. As determining the model evidence requires calculating an integral over the model parameters ( $\theta$ ) which is generally intractable, we approximate it with  $z_0 = z_0(y|M_i)$ , which is based on a second-order Laplace approximation,<sup>34</sup>  $q_0 = q_0(\theta|M_i, y)$ , to the true un-normalised posterior density  $q = q(\theta|M_i, y)$ . The second-order approximated density is estimated as:

$$q_0 = q(\hat{\theta}) \exp \left( -\frac{1}{2} (\theta - \hat{\theta}) \Sigma^{-1} (\theta - \hat{\theta})^T \right). \quad (5)$$

Here  $q(\hat{\theta})$  denotes the value of the un-normalised posterior evaluated using the mean estimates of the model's parameters  $\hat{\theta}$ , and  $\Sigma$  the covariance matrix built from Markov Chain Monte Carlo (MCMC) samples of the posterior distribution. From this expression, a second-order approximation to the model evidence,  $z_0$ , is given by  $z_0 = q(\hat{\theta}) \sqrt{\det(2\pi\Sigma^{-1})}$ , where  $\det(\cdot)$  denotes the deter-

minant of the matrix.

For each model pair, Bayes factors were computed from the marginal likelihoods. Considering two models  $M_i$  and  $M_j$ , the Bayes Factor (BF) is

$$B_{ij} = \frac{z(y|M_i)}{z(y|M_j)}, \quad (6)$$

where  $z(y|M_i)$  is the evidence of model  $M_i$  given  $y$ . If  $B_{ij} > 1$ , the evidence is in favour of model  $M_i$ . Here, for readability we will report the Bayes Factors as  $2 \log(B_{ij})$  following Kass and Raftery notation.<sup>35</sup>

The sensitivity of our model evidence is tested with respect to the choice of hyperprior distribution, and secondly with respect to the use of the approximate second-order density  $q_0$ . In the latter instance this is done by performing thermodynamic integration<sup>21–23</sup> between  $q_0$  and the true density  $q$  in order to obtain an asymptotically exact estimate of the marginal model evidence,

$$z = z_0 \exp \left( \int_0^1 \mathbb{E}_{\theta \sim q(\theta; \lambda)} [\log q - \log q_0] d\lambda \right). \quad (7)$$

The right hand term corrects the  $z_0$  approximation to the exact Bayesian evidence by a path integral evaluated with respect to a sampling distribution that interpolates between the two densities as  $q(\theta; \lambda) = q^{(1-\lambda)} q_0^\lambda$  in terms of the auxiliary coordinate  $\lambda$ .

Table IV. Probability density functions with analytical formulae for mean and variance.  $y$  denotes the data,  $\Gamma(\cdot)$  is a gamma function. GG – generalised gamma, GLN – generalised log-normal.

PDF	Mean	Variance
$\text{Gamma}(y \alpha, \beta) = \frac{\beta^\alpha}{\Gamma(\alpha)} y^{\alpha-1} \exp(-\beta y)$	$\frac{\alpha}{\beta}$	$\frac{\alpha}{\beta^2}$
$\text{Weibull}(y \alpha, \sigma) = \frac{\alpha}{\sigma} \left(\frac{y}{\sigma}\right)^{\alpha-1} \exp\left(-\left(\frac{y}{\sigma}\right)^\alpha\right)$	$\sigma \Gamma\left(1 + \frac{1}{\alpha}\right)$	$\sigma^2 \left(\Gamma\left(1 + \frac{2}{\alpha}\right) - \Gamma^2\left(1 + \frac{1}{\alpha}\right)\right)$
$\text{Log-normal}(y \mu, \sigma) = \frac{1}{\sqrt{2\pi}\sigma} \frac{1}{y} \exp\left(-\frac{1}{2}\left(\frac{\log y - \mu}{\sigma}\right)^2\right)$	$\exp\left(\mu + \frac{\sigma^2}{2}\right)$	$(\exp(\sigma^2) - 1) \exp(2\mu + \sigma^2)$
$\text{GG}(y a, d, p) = \frac{1}{\Gamma\left(\frac{d}{p}\right)} \left(\frac{p}{a}\right)^d x^{d-1} \exp\left(-\left(\frac{y}{a}\right)^p\right)$	$a \frac{\Gamma((d+1)/p)}{\Gamma(d/p)}$	$a^2 \left[ \frac{\Gamma((d+2)/p)}{\Gamma(d/p)} - \left(\frac{\Gamma((d+2)/p)}{\Gamma(d/p)}\right)^2 \right]$
$\text{GLN}(y \mu, \sigma, s) = \frac{1}{y} \frac{s}{2^{\frac{s+1}{s}} \sigma \Gamma\left(\frac{1}{s}\right)} \exp\left(-\frac{1}{2} \left \frac{\log y - \mu}{\sigma}\right ^s\right)$	$\exp(\mu) \left[1 + \frac{1}{2\Gamma(1/s)} \cdot S\right],$ $S = \sum_{j=1}^{\infty} \sigma^j \left(1 + (-1)^j\right) 2^{j/s} \frac{\Gamma\left(\frac{j+1}{2}\right)}{\Gamma(j+1)}$	$\exp(2\mu) \left[1 + \frac{1}{2\Gamma(1/s)} \cdot S\right] - [\text{Mean}]^2,$ $S = \sum_{j=1}^{\infty} 2\sigma^j \left(1 + (-1)^j\right) 2^{j/s} \frac{\Gamma\left(\frac{j+1}{2}\right)}{\Gamma(j+1)}$

Table V. Bayes Factors (BFs) for the analysed distributions and models. For each distribution (rows), the values represent BF for the best fitting model against other models. Value of 0 indicates the model that fits the data the best. Value  $> 10$  indicates a very strong evidence against given model compared to the best one. GLN - generalised log-normal, GG - generalised gamma. NA - not analysed. The BF values are reported here as  $2 \log(B_{ij})$  following Kass and Raftery notation.<sup>35</sup>

	Gamma	Weibull	Log-normal	GLN	GG
Onset-to-death	0	2156	2208	198	301
Admission-death	0	195	4349	3096	188
ICU stay	0	231	588	607	352
Onset-to-hospital-admission	4000	17073	494	0	NA
Onset-to-hospital-discharge	2819	8346	6079	0	3087
Onset-to-ICU-admission	798	4359	142	0	1244
Onset-to-diagnosis (PCR)	1111	10400	13882	0	1257
Onset-to-diagnosis (non-PCR)	578	793	4340	0	461

Table VI. State-level onset-to-death estimates for gamma PDF: mean, variance, parameters values, with 95% confidence intervals. The parameters  $p_1$  and  $p_2$  are given in the form  $\text{Gamma}(x|p_1, p_2) = \text{Gamma}(\alpha, \beta)$ . The full PDFs for other distributions are available at [https://github.com/mrc-ide/Brazil\\_COVID19\\_distributions/blob/master/results/results\\_full\\_table.csv](https://github.com/mrc-ide/Brazil_COVID19_distributions/blob/master/results/results_full_table.csv).

State	Mean (days)	Variance (days <sup>2</sup> )	$p_1$	$p_2$
AC	17.4 (16.1, 18.8)	119.4 (98.8, 143.6)	2.6 (2.2, 2.9)	0.1 (0.1, 0.2)
AL	14.0 (13.4, 14.5)	82.5 (74.3, 91.9)	2.4 (2.2, 2.5)	0.2 (0.2, 0.2)
AM	15.6 (15.3, 16.0)	95.3 (89.1, 102.1)	2.6 (2.4, 2.7)	0.2 (0.2, 0.2)
AP	14.5 (13.2, 16.0)	99.1 (79.8, 122.7)	2.1 (1.9, 2.4)	0.1 (0.1, 0.2)
BA	15.1 (14.7, 15.6)	116.6 (107.9, 126.1)	2.0 (1.9, 2.1)	0.1 (0.1, 0.1)
CE	16.1 (15.8, 16.4)	116.4 (111.1, 122.0)	2.2 (2.2, 2.3)	0.1 (0.1, 0.1)
DF	16.4 (15.6, 17.2)	105.0 (92.7, 119.0)	2.6 (2.3, 2.8)	0.2 (0.1, 0.2)
ES	17.0 (16.4, 17.5)	107.8 (98.2, 118.1)	2.7 (2.5, 2.9)	0.2 (0.1, 0.2)
GO	14.5 (13.8, 15.2)	87.9 (77.9, 99.1)	2.4 (2.2, 2.6)	0.2 (0.2, 0.2)
MA	15.0 (14.6, 15.4)	89.4 (82.7, 96.5)	2.5 (2.4, 2.7)	0.2 (0.2, 0.2)
MG	15.1 (14.6, 15.7)	95.1 (86.3, 104.7)	2.4 (2.2, 2.6)	0.2 (0.1, 0.2)
MS	14.8 (13.3, 16.4)	93.9 (74.8, 116.8)	2.4 (2.0, 2.7)	0.2 (0.1, 0.2)
MT	14.1 (13.1, 15.1)	80.6 (67.2, 96.4)	2.5 (2.2, 2.8)	0.2 (0.2, 0.2)
PA	14.7 (14.5, 15.0)	90.2 (85.7, 94.9)	2.4 (2.3, 2.5)	0.2 (0.2, 0.2)
PB	14.0 (13.4, 14.5)	78.7 (71.2, 87.3)	2.5 (2.3, 2.7)	0.2 (0.2, 0.2)
PE	13.0 (12.7, 13.2)	89.7 (84.6, 95.1)	1.9 (1.8, 1.9)	0.1 (0.1, 0.2)
PI	16.5 (15.6, 17.4)	114.8 (99.4, 131.7)	2.4 (2.1, 2.6)	0.1 (0.1, 0.2)
PR	15.7 (15.1, 16.4)	91.9 (81.8, 102.7)	2.7 (2.5, 2.9)	0.2 (0.2, 0.2)
RJ	14.2 (14.0, 14.4)	103.3 (99.5, 107.3)	2.0 (1.9, 2.0)	0.1 (0.1, 0.1)
RN	15.2 (14.6, 15.9)	91.9 (81.8, 103.0)	2.5 (2.3, 2.7)	0.2 (0.2, 0.2)
RO	14.7 (13.6, 15.8)	92.1 (76.4, 110.0)	2.3 (2.1, 2.6)	0.2 (0.1, 0.2)
RR	11.2 (10.2, 12.1)	68.1 (55.9, 83.0)	1.8 (1.6, 2.1)	0.2 (0.1, 0.2)
RS	15.4 (14.7, 16.2)	116.0 (103.0, 130.8)	2.1 (1.9, 2.2)	0.1 (0.1, 0.1)
SC	17.8 (16.7, 19.0)	146.8 (125.1, 173.5)	2.2 (1.9, 2.4)	0.1 (0.1, 0.1)
SE	13.4 (12.2, 14.5)	112.5 (91.4, 138.6)	1.6 (1.4, 1.8)	0.1 (0.1, 0.1)
SP	16.2 (16.0, 16.4)	114.8 (111.6, 118.0)	2.3 (2.2, 2.3)	0.1 (0.1, 0.1)
TO	14.8 (13.5, 16.2)	97.3 (79.1, 119.7)	2.3 (2.0, 2.6)	0.2 (0.1, 0.2)
Brazil	15.2 (15.1, 15.3)	105.3 (103.7, 106.9)	2.2 (2.2, 2.2)	0.1 (0.1, 0.1)

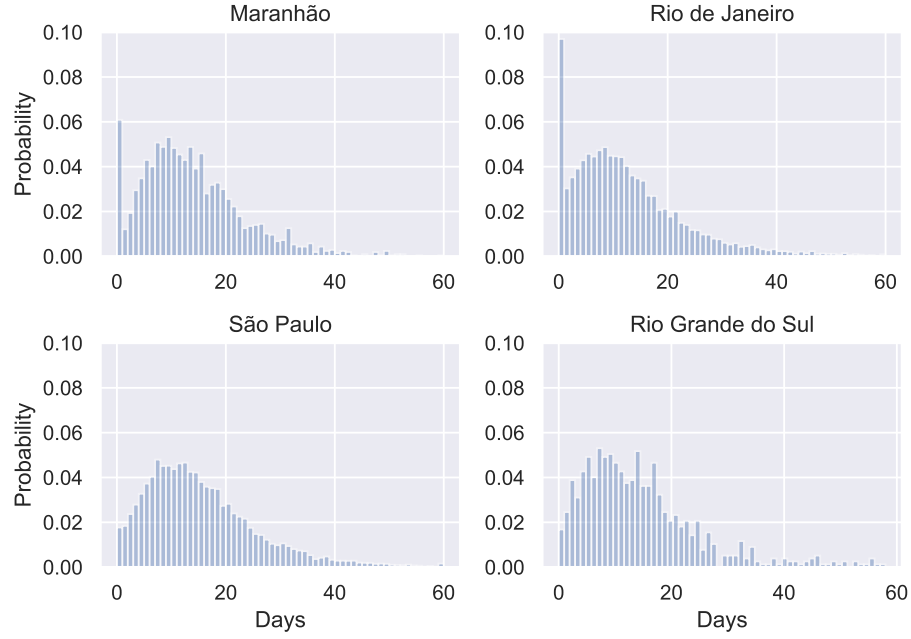


Figure 4. Distribution of onset-to-death for Maranhão, Rio de Janeiro, So Paulo and Rio Grande do Sul. Anomalous spikes for the first day can be observed for Maranhão and Rio de Janeiro, indicating they might be a reporting error.

Table VII. Pearson correlation coefficients for mean distribution times and socioeconomic indicators. Sample size was equal to 27 (number of states).

	ICU-stay	Onset-death	Admission-death	Onset-discharge	Onset-hospital admission	Onset-ICU admission	Onset-diagnosis (PCR)
Education	-0.32	-0.25	-0.62	0.41	0.48	0.39	0.34
Poverty	-0.31	-0.31	-0.68	0.52	0.69	0.54	0.49
Deprivation	0.38	0.35	0.71	-0.49	-0.59	-0.49	-0.41
Wealth	-0.08	0.26	0.37	-0.24	-0.07	-0.21	-0.17
Income	0.21	0.28	0.60	-0.35	-0.40	-0.33	-0.35
Segregation	0.40	0.35	0.62	-0.43	-0.57	-0.47	-0.30
Mean age	0.13	0.25	0.43	-0.45	-0.57	-0.68	-0.25
Urbanicity	0.12	0.11	0.43	-0.34	-0.52	-0.40	-0.19

Table VIII. Pearson correlation coefficients for mean distribution times. Sample size was equal to 27 (number of states).

	Onset-death	Admission-death	Onset-discharge	Onset-hospital admission	Onset-ICU admission	Onset-diagnosis (PCR)
Onset-death	1	0.69	-0.35	0.06	0.24	0.15
Admission-death	0.69	1	-0.52	-0.48	-0.20	-0.36
Onset-discharge	-0.35	-0.52	1	0.39	0.43	0.40
Onset-to-hospital-admission	0.06	-0.48	0.39	1	0.72	0.53
Onset-to-ICU-admission	0.24	-0.20	0.43	0.72	1	0.50
Onset-to-diagnosis (PCR)	0.15	-0.36	0.40	0.53	0.50	1

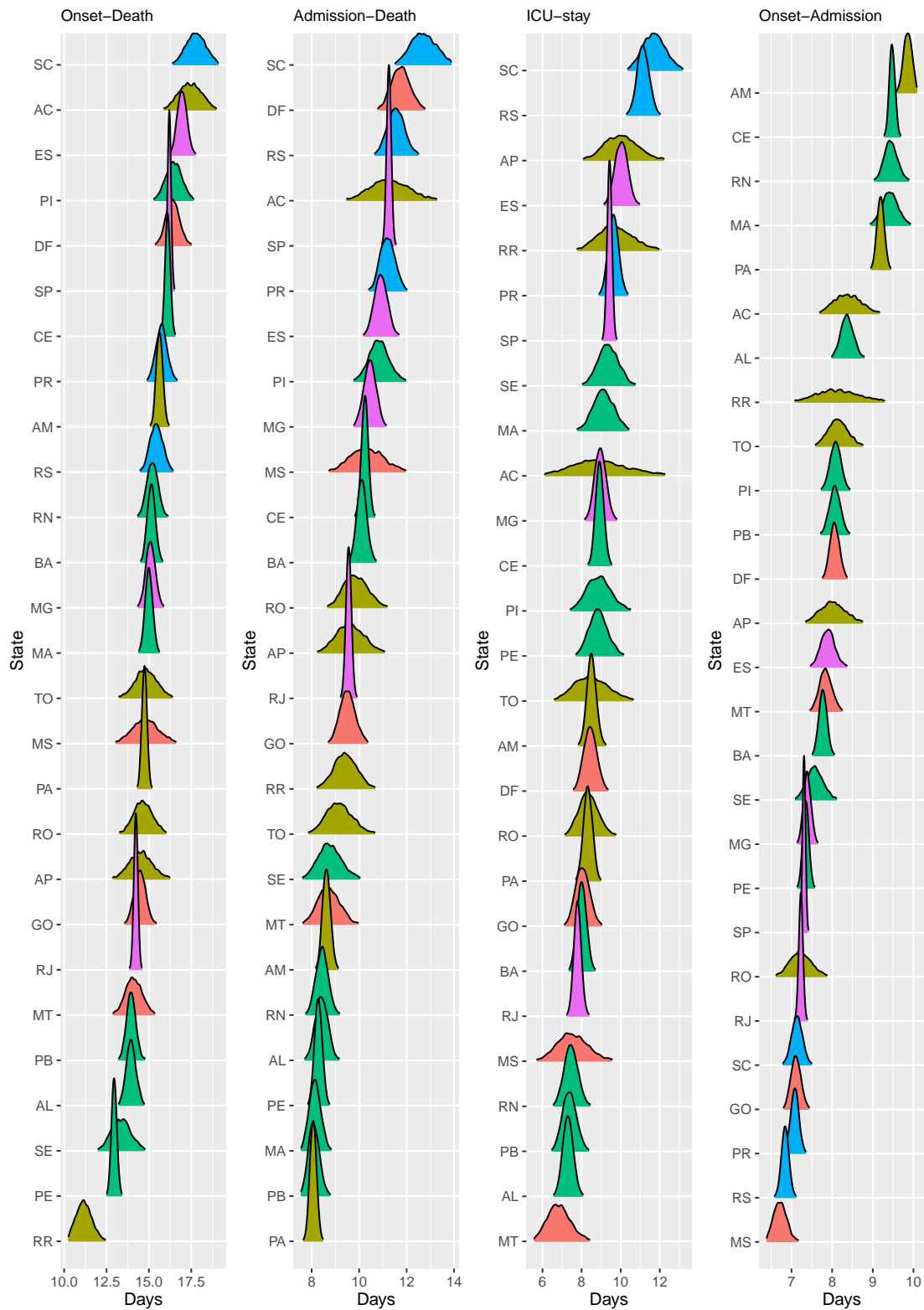


Figure 5. Posterior distribution of mean times (in days) for onset-to-death, hospital-admission-to-death, ICU stay and onset-to-hospital-admission, sorted by mean value. Plots are colour-coded by the geographical region which the state belongs to: North (yellow), Northeast (green), Central-West (orange), Southeast (purple), South (blue).

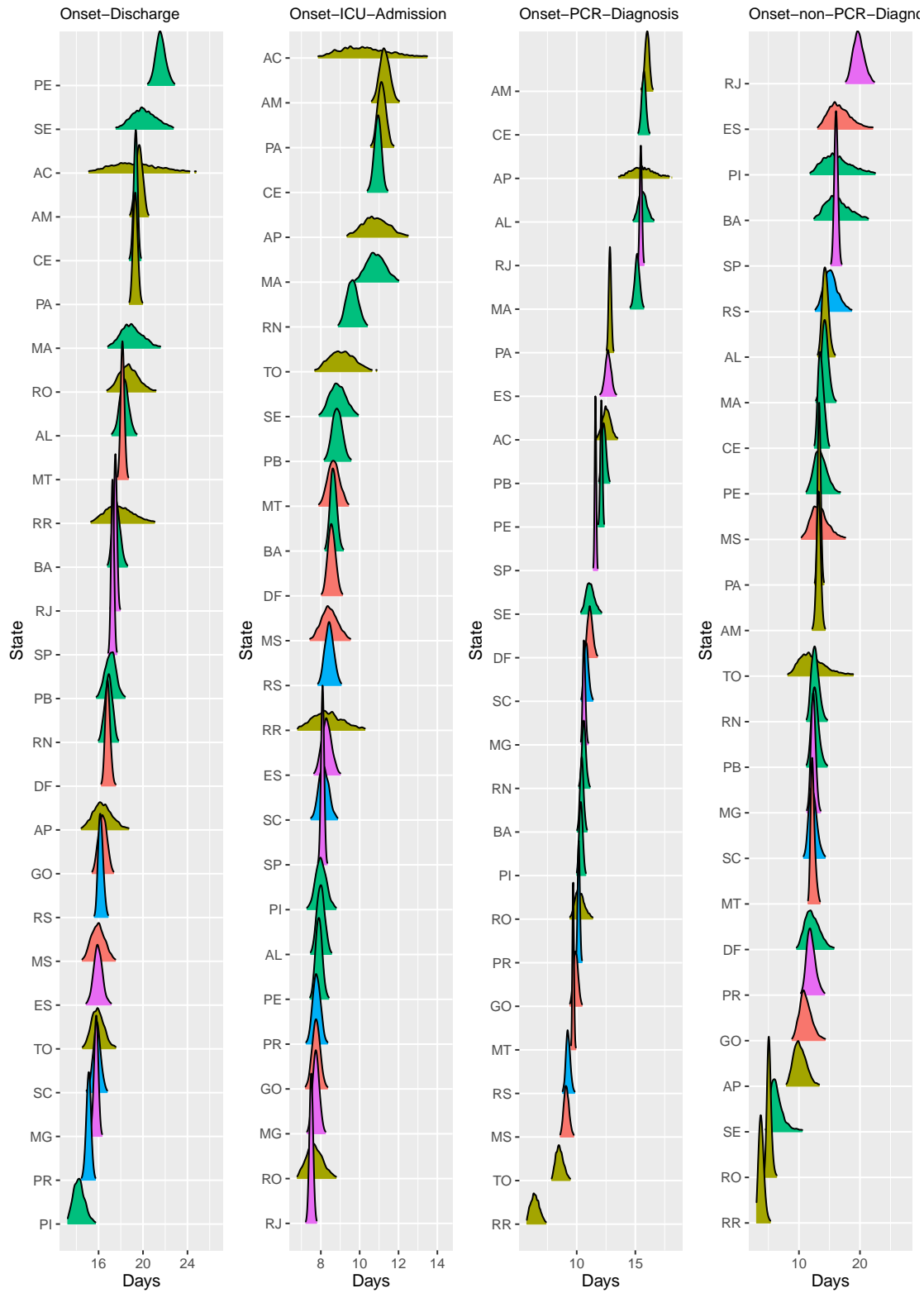


Figure 6. Posterior distribution of mean times (in days) for onset-to-hospital-discharge, onset-to-ICU-admission, onset-to-diagnosis (PCR) and onset-to diagnosis (non-PCR), sorted by mean value. Plots are colour-coded by the geographical region which the state belongs to: North (yellow), Northeast (green), Central-West (orange), Southeast (purple), South (blue).

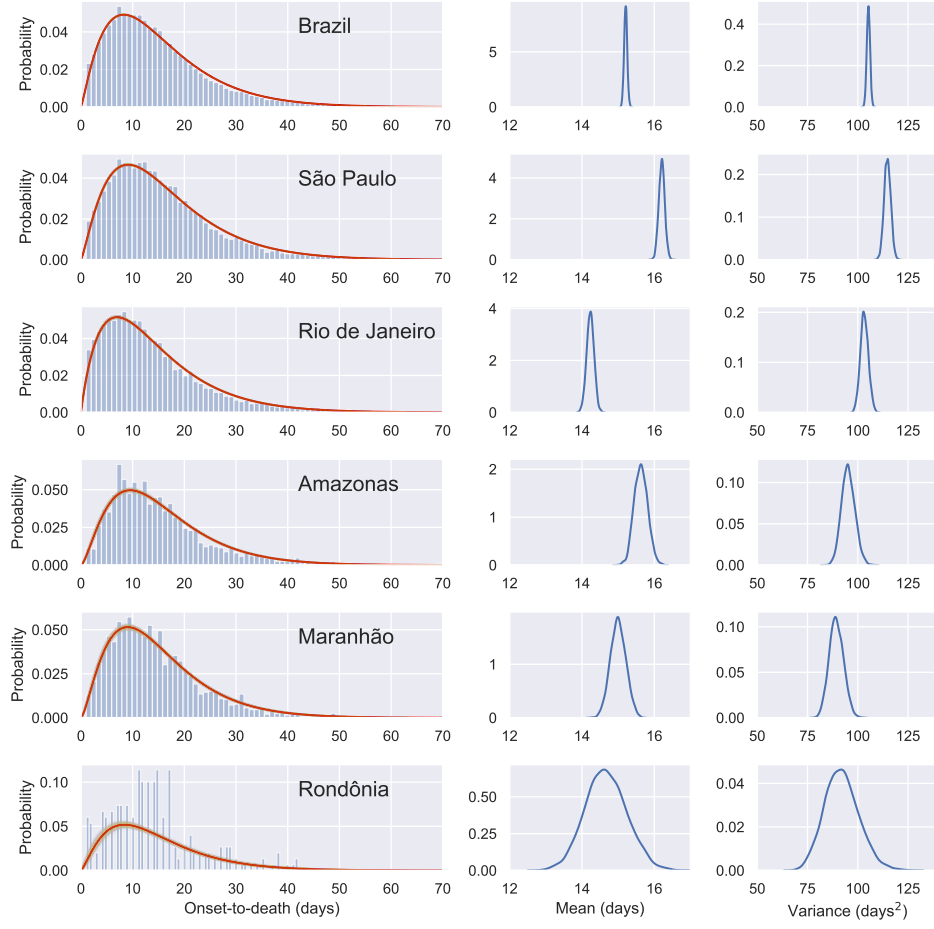


Figure 7. Gamma PDF  $\text{Gamma}(\alpha, \beta)$  fitted to the onset-to-death data for Brazil and five states of Brazil. The PDFs were fitted with HMC partially pooling each state with the whole country. The red lines represent the model using the mean parameter estimates. Individual PDFs selected during MCMC sampling are shown in yellow. Posterior mean and variance distributions for each region are given in the middle and right hand side columns.

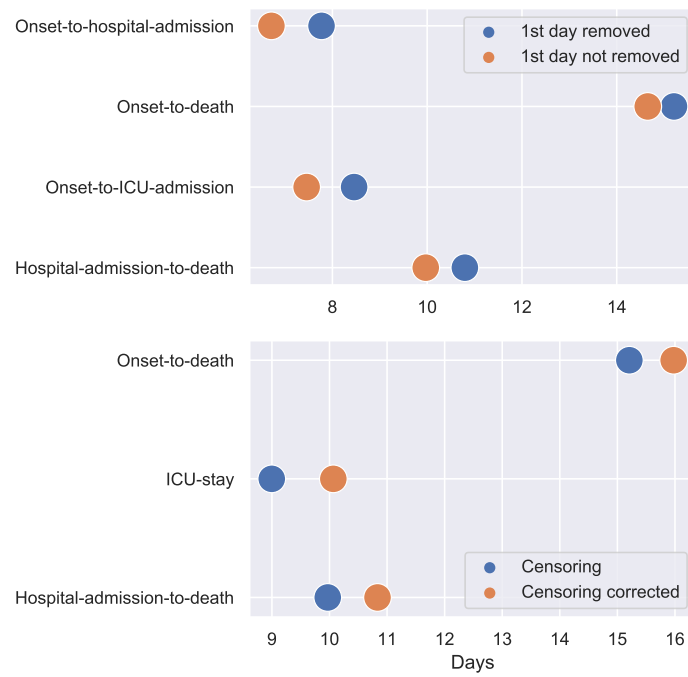


Figure 8. Estimated mean per distribution in different scenarios: excluding 1st day data points (top) and censoring correcting (bottom). The credible intervals were not shown as due to the large amount of data available they were negligible.



Table IX. Number of datapoints per state for each of the datasets analysed in the study. Acre (AC), Amazonas (AM), Amap (AP), Par (PA), Rondonia (RO), Roraima (RR), Tocantins (TO), Alagoas (AL), Bahia (BA), Cear (CE), Maranhão (MA), Paraíba (PB), Piauí (PI), Pernambuco (PE), Sergipe (SE), Rio Grande do Norte (RN), Distrito Federal (DF), Goiás (GO), Mato Grosso do Sul (MS), Mato Grosso (MT), Espírito Santo (ES), Minas Gerais (MG), Rio de Janeiro (RJ), São Paulo (SP), Paraná (PR), Rio Grande do Sul (RS), Santa Catarina (SC).

	Onset-death	Admission-Death	ICU-stay	Onset-hospital admission	Onset-hospital discharge	Onset-ICU admission	Onset-diagnosis (PCR)	Onset-diagnosis (non-PCR)
AC	239	115	2	225	4	9	345	1
AL	1040	894	680	1600	629	859	1344	416
AM	2736	2403	1010	5971	2573	1323	4502	1604
AP	181	175	68	299	136	80	183	153
BA	2241	2013	982	4563	1338	2300	5266	352
CE	5801	4905	1534	9685	4536	2768	8286	1749
DF	662	655	499	2687	1415	1198	2864	311
ES	1292	1023	589	1409	507	778	1774	321
GO	698	637	375	1813	783	819	2018	122
MA	1950	1097	197	1485	247	341	1562	821
MG	1223	1176	603	4782	2210	1521	4910	604
MS	131	124	46	723	417	171	764	126
MT	286	248	83	1347	2191	384	4695	2175
PA	4727	3934	1270	8226	3034	1993	6921	1351
PB	1136	1037	349	1992	508	740	1584	644
PE	4408	3284	311	6574	1888	1566	9745	190
PI	515	497	139	2161	341	490	2314	240
PR	793	773	898	3174	1952	1168	3490	124
RJ	9750	9068	1490	18019	7438	7165	21159	1446
RN	876	821	337	1878	664	693	1517	544
RO	254	238	180	554	180	284	488	293
RR	270	265	53	98	51	56	200	92
RS	790	770	971	3565	2328	1277	4144	477
SC	408	389	291	1600	777	599	1634	343
SE	303	295	193	938	181	306	1116	117
SP	16348	15808	8515	55735	32937	17642	63184	4769
TO	213	177	44	515	213	87	549	53